Enhancing optical response of graphene through stochastic resonance

Lei Ying, Liang Huang, and Ying-Cheng Lai

Phys. Rev. B **97**, 144204 — Published 30 April 2018

DOI: 10.1103/PhysRevB.97.144204

Enhancing optical response of graphene through stochastic resonance

Lei Ying,[1] Liang Huang,[2] and Ying-Cheng Lai[1,3,*]

[1]*School of Electrical, Computer, and Energy Engineering, Arizona State University, Tempe, Arizona 85287, USA*

[2]*School of Physical Science and Technology, and Key Laboratory for Magnetism and Magnetic Materials of MOE, Lanzhou University, Lanzhou, Gansu 730000, China*

[3]*Department of Physics, Arizona State University, Tempe, Arizona 85287, USA*

To enhance the optical response of graphene is a topic of interest with applications to optoelectronics. Subject to light irradiation, graphene can exhibit non-trivial topologically insulating states, effectively turning itself into a Floquet topological insulator due to the time periodicity of the external driving. We find that, when random disorder is present, its interplay with the topologically insulating states can have a dramatic effect on electronic transport through graphene. In particular, we consider the prototypical setting where a graphene nanoribbon is irradiated by circularly polarized light, where the length of the nanoribbon is sufficiently long so that evanescent states have little effect on transport. We uncover a resonance phenomenon, in which the conductance is enhanced as the disorder strength is increased from zero, reaches a maximum value for an optimal level of disorder, and decreases as the disorder is strengthened further. With respect to its value at the zero disorder strength, the maximum conductance value can be as much as 50% higher. Qualitatively, this can be understood as a result of the dynamical interplay between disorder and Floquet states (channels) generated by light irradiation. Quantitatively, the resonance phenomenon can be explained in the framework of Born theory, where the disorder reorganizes the Floquet Hamiltonian and enhances the effective coupling between the adjacent Floquet conducting channels. That is, disorder is capable of promoting both photon absorption and emission, leading to significant enhancement of nonequilibrium electronic transport. We demonstrate the robustness of the resonance phenomenon by investigating the effects of spatial symmetry breaking on transport and provide an understanding based on analyzing the behavior of the density of states of the Floquet channels.

I. INTRODUCTION

The optical absorption of monolayer graphene is determined exclusively by the fine structure constant α and has little dependence on the frequency in a wide spectral range, as a consequence of the low-energy electronic structure in which the electron and hole conical bands meet each other at the Dirac point in a linear fashion. The value of the absorption is thus low: about $\pi\alpha \approx 2.3\%$ for a wide frequency range containing the visible spectrum[1–4], making graphene effectively "transparent" to light. With conventional methods such as electrostatic gating and doping, light absorption in graphene can be improved but not dramatically. For applications in optoelectronics, it is of interest to enhance the response of graphene to light even without significant enhancement in absorption. In this paper, we report a stochastic resonance phenomenon[5–12] by which the interplay between light irradiation and random disorder can maximize the conductance through a graphene nanoribbon.

When an external light beam irradiates on a graphene-like or a spin-orbit coupled system, dynamical and topologically insulating states can arise[13]. Such nontrivial states with time-periodic variations can be described by the Floquet theory - henceforth the term *Floquet topological insulators* (FTIs). Subsequently, various properties of FTIs and the associated phenomena have been studied theoretically and computationally, such as transport[14–17], edge states[18–21], topological transitions[22,23], dynamical polarizability[24], modulated and disorder-induced topological states[25–27], valleytronics[28], and local pseudospin textures[29]. Experimental observation of Floquet-Bloch states on the surface of a topological insulator[30] has also been reported.

Transport dynamics in Floquet systems are of the nonequilibrium nature[14,31] due to the time-dependent external light field, leading to behaviors that are distinct from those in equilibrium transport systems. For example, a short, light-irradiated graphene ribbon can exhibit a superdiffusive behavior caused by the evanescent modes[32]. In a light-irradiated bulk graphene system, the phenomenon of disorder-enhanced transport can arise[22] through breaking of the spatiotemporal symmetry. This should be compared with non-irradiated systems, where disorder-enhanced transport assisted by evanescent states can be observed in short structures[33–35] or in systems with pointer states induced by specific mechanisms such as scattering sources[36,37] or an external magnetic field[38]. Earlier, a stochastic resonance phenomenon was uncovered[39,40] whereby the transmission through a disordered graphene nanojunction can be maximized for an optimal level of random disorder. This can be understood as the breaking of the localized edge states by weak impurities, resulting in enhanced transmission, but strong disorder can lead to Anderson localization, reducing the conductance. From the standpoint of scatter-

ing, the effects of random impurities are similar to those of classical chaos[41], indicating that chaos can play a role in modulating quantum transmission[42–51]. In previous works on the effects of random impurities on transport in graphene nanoribbons, the disorder enhanced conductance is typically small: $\Delta G \ll G_0 = 2e^2/h$. We also note that bulk transport is not completely representative of transport dynamics in the ribbon structure.

In this paper, we study transport through a light-irradiated graphene ribbon structure with on-site disorders, which is connected with two doped leads. We focus on the weak-disorder regime for consideration that FTIs are typically weak topological insulators[52,53]. We study the setting where a circularly polarized light beam irradiates a sufficiently long graphene ribbon so that evanescent states have no contribution to the transport. We find that on-site disorder can enhance the transport. As the disorder strength is increased, the conductance can increase and reach a maximum at some optimal value of the disorder strength, mimicking a stochastic resonance. This resonance phenomenon is robust with respect to variations in other parameters of the system. We develop a theory based on the Born approximation to understand the mechanism for resonance. Our analysis indicates that disorder can effectively enhance the coupling between light and graphene with respect to photon absorption or emission. We also consider symmetry breaking by assuming that there is only partial disorder in the system, find persistence of the resonance phenomenon, and offer an explanation based on analyzing density of states in different Floquet channels. While disorder has been known to be capable of enhancing electronic transport in graphene ribbon in the absence of external light, our work reveals, quite surprisingly, that the interaction between electromagnetic radiation and graphene can be significantly enhanced when certain amount of disorder is present.

II. NONEQUILIBRIUM TRANSPORT AND FLOQUET THEORY

For a graphene ribbon subject to uniform, circularly polarized light irradiation, the time-dependent Hamiltonian under the unit convention $\hbar = v_F = 1$ is given by $H(t) = H_0 + H_1[\mathbf{A}(t)]$, where H_0 is the unperturbed Hamiltonian in the absence of light, $H_1[\mathbf{A}(t)]$ is the perturbation term due to the vector potential $\mathbf{A}(t) = (eA_0/\hbar)[\cos(\Omega t), \sin(\Omega t)]$ that characterizes the effect of the rotating electric field in the (x, y) plane: $\mathbf{E}(t) = -\partial\mathbf{A}(t)/\partial t$ with Ω being the frequency of light and A_0 being a quantity related to the light intensity. The time-dependent Schrödinger equation is

$$\mathcal{H}_F(t)|\Psi(\mathbf{r},t)\rangle = [H(t) - i\partial_t]|\Psi(\mathbf{r},t)\rangle = 0, \qquad (1)$$

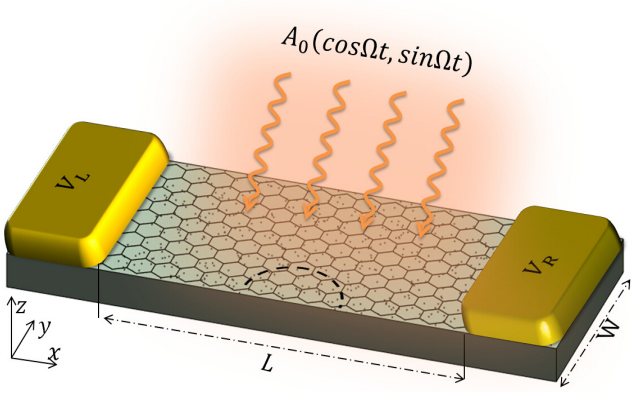

FIG. 1. **Schematic illustration of system configuration**. A two-terminal graphene nanoribbon of length L and width W is irradiated by a circularly polarized light beam of strength A_0 and frequency Ω. The random black dots denote the on-site potential disorder. The left and right leads are shielded from light irradiation by the electrodes. The quantities $V_{L,R}$ represent the potential at the left and right lead, respectively.

where $\mathcal{H}_F(t)$ is the Floquet Hamiltonian[15]. Since $H(t)$ is periodic, the wavefunction can be expressed as the Floquet states $|\Psi_\alpha(\mathbf{r},t)\rangle = e^{i\varepsilon_\alpha t}|\Phi_\alpha(\mathbf{r},t)\rangle$, where ε_α is the quasienergy and $|\Phi_\alpha(\mathbf{r},t+T)\rangle = |\Phi_\alpha(\mathbf{r},t)\rangle$ with $T = 2\pi/\Omega$ being the driving period. The Schrödinger equation can then be reduced to $\mathcal{H}_F(t)|\Phi_\alpha(\mathbf{r},t)\rangle = \varepsilon_\alpha|\Phi_\alpha(\mathbf{r},t)\rangle$. The wavefunction can be expressed in the discrete Fourier form as

$$|\Phi_\alpha(\mathbf{r},t)\rangle = \sum_m e^{im\Omega t}|\varphi_\alpha^m(\mathbf{r})\rangle, \qquad (2)$$

where $|\varphi_\alpha^m(\mathbf{r})\rangle$ is static. Since $\mathcal{H}_F$ is Hermitian, the Floquet states $|\Phi_\alpha(\mathbf{r},t)\rangle$ are orthonormal to each other[26]:

$$\sum_m \langle\varphi_\alpha^m|\varphi_\beta^m\rangle = \delta_{\alpha\beta}.$$

In the tight-binding framework, the time-dependent Hamiltonian is given by

$$H(t) = -\sum_{\langle ij\rangle,s} \gamma_{ij}(t)c_{i,s}^\dagger c_{j,s} + \sum_{i,s} u_i c_{i,s}^\dagger c_{i,s}, \qquad (3)$$

where $c_{i,s}^\dagger(c_{i,s})$ is the creation(annihilation) operator, $s = \uparrow, \downarrow$ denotes spin, and u_i is the on-site disorder potential at site i. The manifestation of the light field is the following dependence of the hopping energy on the vector potential:

$$\gamma_{ij} = \gamma_0 \exp[iA_{ij}(t)],$$

where

$$A_{ij}(t) = (e/\hbar)(\mathbf{r}_j - \mathbf{r}_i)\cdot\mathbf{A}.$$

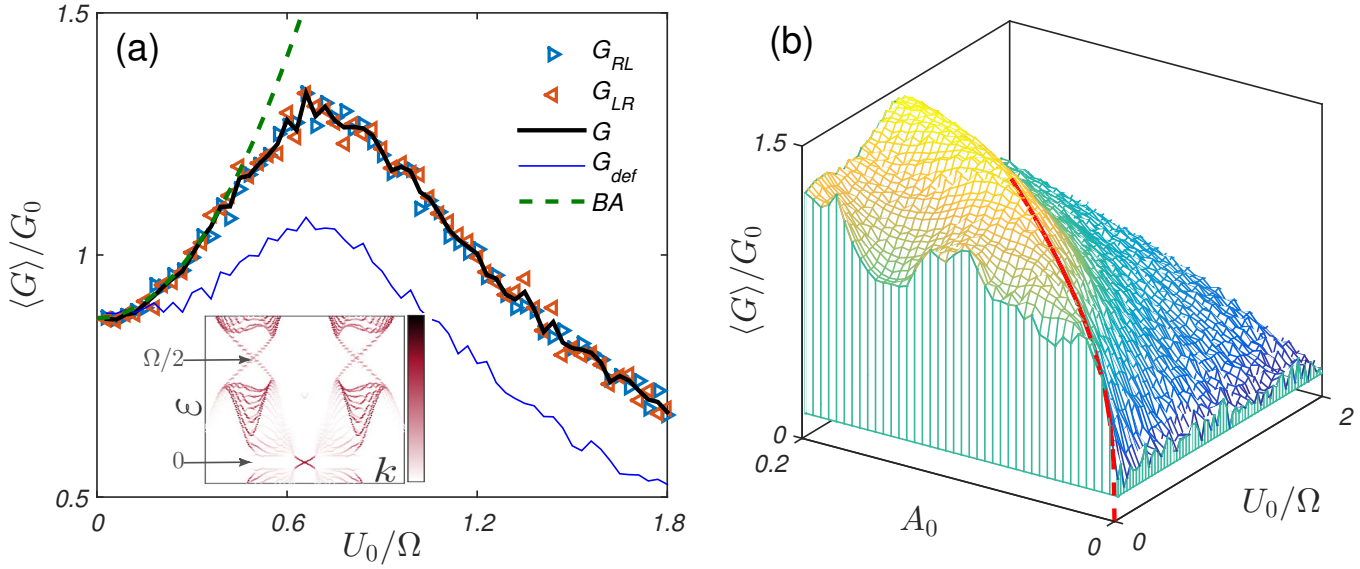

FIG. 2. **Main result: enhancement of conductance by light-disorder interplay**. Under relatively weak light irradiation, (a) average conductance $\langle G\rangle$ versus the disorder strength U_0. Blue rightward and red leftward triangles denote the conductance associated with transport in the $L \to R$ and $R \to L$ direction, respectively. The black curve corresponds to the mean conductance G. The quantity G_{defect}, represented by the blue curve, is the conductance for the case where impurities are distributed uniformly in a semicircular region of radius $r = W/2$, as indicated in Fig. 1. The green dashed curve is the theoretical prediction based on the Born approximation. The arrows at $\varepsilon = 0$ and $\Omega/2$ in the inserted quasienergy band structure correspond to the FTI states. The parameters are $L = 70a_0$, $W = 50a$, $A_0 = 0.15$ and $\Omega = 0.8\gamma_0$, with $a_0 = \sqrt{3}a = 2.46$Å being the lattice constant of graphene. The convention that $\hbar = 1$ has been used. (b) Average conductance versus A_0 and U_0. The red curve is a fit with the conductance peaks.

The value of the random potential u_i is taken from a uniform distribution in the interval $[-U_0/2, U_0/2]$ with $\langle u_i\rangle = 0$ and $\langle u_i u_j\rangle = (U_0^2/12)\delta_{ij}$.

We study a two-terminal transport system, as shown in Fig. 1, where the "scattering" region is irradiated by a circularly polarized light beam. In experiments, the left and right leads are typically covered by electrodes and are thus not irradiated. This is a non-equilibrium transport system due to photon absorption and emission, where electrons are injected from the left lead with Fermi energy E, interact with light in the scattering region, and exit from either the left or the right lead with energy $E + k\hbar\Omega$, where k is the number of photons absorbed or emitted. The zero-temperature conductance can be obtained from the non-equilibrium Green's function method as $G = (G_{RL} + G_{LR})/2$, where

$$G_{\nu\leftarrow\mu}(E) \equiv G_{\nu\mu}(E) = G_0 \sum_k T_{\nu\mu}^{(k)}(E) \text{ and}$$

$$T_{\nu\mu}^{(k)}(E) = Tr[\Gamma_\nu^{(k)} \mathcal{G}_{1N}^{(k)}(E) \Gamma_\mu^{(0)} \mathcal{G}_{1N}^{(k)\dagger}(E)].$$

See Appendix A for a detailed description of the computational method.

III. RESULTS

A. Light mediated, disorder enhanced transport

To calculate the conductance of the irradiated region, we assume that the leads are doped to increase the number of transverse modes injected from the leads into the scattering region. Computationally, this can be implemented by setting the potentials at the left and right leads as $V_L = V_R = \gamma_0$. To eliminate the effect of evanescent states, we set the length-to-width ratio of the scattering region to be $L/W \gtrsim 2.5$. We use the notation G to represent the time averaged conductance, whereas the notation $\langle\cdots\rangle$ is reserved for ensemble average over the disorder configurations.

Figure 2(a) shows the average conductance versus the disorder strength, which exhibits a resonance phenomenon: there exists an optimal value of the disorder strength U_0 which maximizes the conductance. In particular, as U_0 is increased from zero, the average conductance increases, reaches maximum for $U_0/\Omega \approx 0.7$, and decreases monotonically from the maximum value as U_0 is increased further. Note that, when the disorder is uniformly distributed, there is a right-left symmetry in the system, leading to $\langle G_{RL}\rangle = \langle G_{LR}\rangle$. However, the resonance phenomenon persists when such a symmetry is not

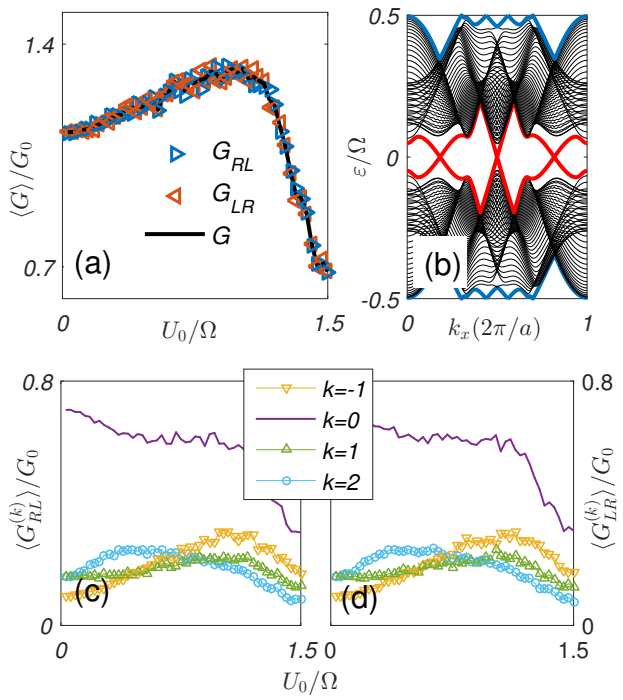

FIG. 3. **Enhancement of conductance by random disorder in the regime of strong light intensity**. (a) Average conductance $\langle G\rangle$ versus the disorder strength U_0. Blue rightward and red leftward triangles denote G_{RL} and G_{LR}, respectively. The black curve corresponds to the average conductance $G = (G_{RL} + G_{LR})/2$. The parameters are $L = 122a$, $W = 50a$, $A_0 = 1$, and $\Omega = 1.533\gamma_0$. (b) The corresponding Floquet spectrum, where the red and blue curves correspond to the FTI states. (c,d) Floquet conductances $G^{(k)}_{RL}$ and $G^{(k)}_{LR}$ versus U_0/Ω, respectively.

present. For example, we have also studied a nanoribbon with impurities uniformly distributed in a semicircular region indicated by the black dashed curve in Fig. 1, and found a similar behavior in the conductance.

To better understand the effects of the interplay between irradiated light and random disorder on electronic transport, we generate a diagram of conductance versus both A_0 and U_0, as shown in Fig. 2(b). In the absence of light ($A_0 = 0$), the conductance remains at near zero values as the disorder strength is varied. When irradiated light even of low intensity is present, a nontrivial FTI state is induced and the conductance rapidly rises to a value about the order of magnitude of G_0 as the disorder strength is increased from zero. The reason that the conductance enhancement is insignificant in the regime of low light intensity is that the FTI state is not robust and the impurities induce a localization effect, resulting in a decrease in the conductance as U_0 is increased further. For relatively strong light intensity, e.g., $A_0 > 0.04$, impurities can lead to considerable conductance enhancement. We find that the maximum conductance $G_{\max}$ obeys the following scaling relation with the light intensity: $G_{\max} \sim A_0^{1/3}$. In the (A_0, U_0) parameter plane, the locations at which $G_{\max}$ is achieved constitute approximately a straight line given by $U_0/\Omega - 5A_0 = 0$.

Previously it was found that, associated with bulk transport through a graphene nanoribbon, disorder-enhanced conductance is due to the breaking of the entwined spatiotemporal symmetry at the Γ point[22]. In our system, the substantial disorder-enhanced conductance in a zigzag ribbon occurs not only at the Γ point but for a range of the intensity of light irradiation (e.g., $A_0 < 0.5$). Even for strong light intensity (e.g., $A_0 \gtrsim 1$), the phenomenon of disorder-enhanced conductance persists, as exemplified in Fig. 3.

For a graphene ribbon with zigzag boundaries, the phenomenon of light mediated, disorder-enhanced transport typically occurs near the quasienergy level $\varepsilon/\Omega = N/2$, where N is an integer. If the quasienergy of the irradiated region is close to the levels of the bulk states, random impurities will weaken or even block the transport, due to the sensitivity of the bulk states to weak disorder. Thus, the phenomenon can arise only when the quasienergy level is distinct from the bulk levels. Another constraint is that the light frequency Ω should be less than the tight-binding bandwidth, for otherwise the conductance will remain at a value in the weak disorder regime. Numerically, we find that the boundary type of the graphene nanoribbon does not affect the emergence of the phenomenon of light-disorder interplay induced conductance enhancement. For example, for the armchair boundaries, we observe similar behaviors.

B. Theoretical understanding based on the Born approximation

To understand the phenomenon of enhanced transport caused by the interplay between disorder and light irradiation, we exploit the first-order Born approximation by starting from the standard single-resonance Hamiltonian in the low energy regime and incorporating random disorder to obtain an effective Hamiltonian. The average self-energy associated with the disorder can be written as[27]

$$\Sigma_{dis}(z, \mathbf{k}) = \int_{FBZ} d\mathbf{k}' \langle U_{dis}(\mathbf{k}, \mathbf{k}') G_0^F(z, \mathbf{k}') U_{dis}(\mathbf{k}', \mathbf{k}) \rangle, \tag{4}$$

where "FBZ" stands for the first Brillouin zone and the off-diagonal elements represent the coupling between different Floquet channels. For weak light irradiation, i.e., $A_0 \ll 1$, the effective coupling strength is

$$\widetilde{A}_{\pm} = A_0(1 + \alpha_{\pm} U_0^2), \tag{5}$$

where $\alpha_{\pm}(\Omega, A_0)$ is an integral over the FBZ with the relation $\alpha_+ = \alpha_-^{\dagger}$. The disorder self-energy indicates that

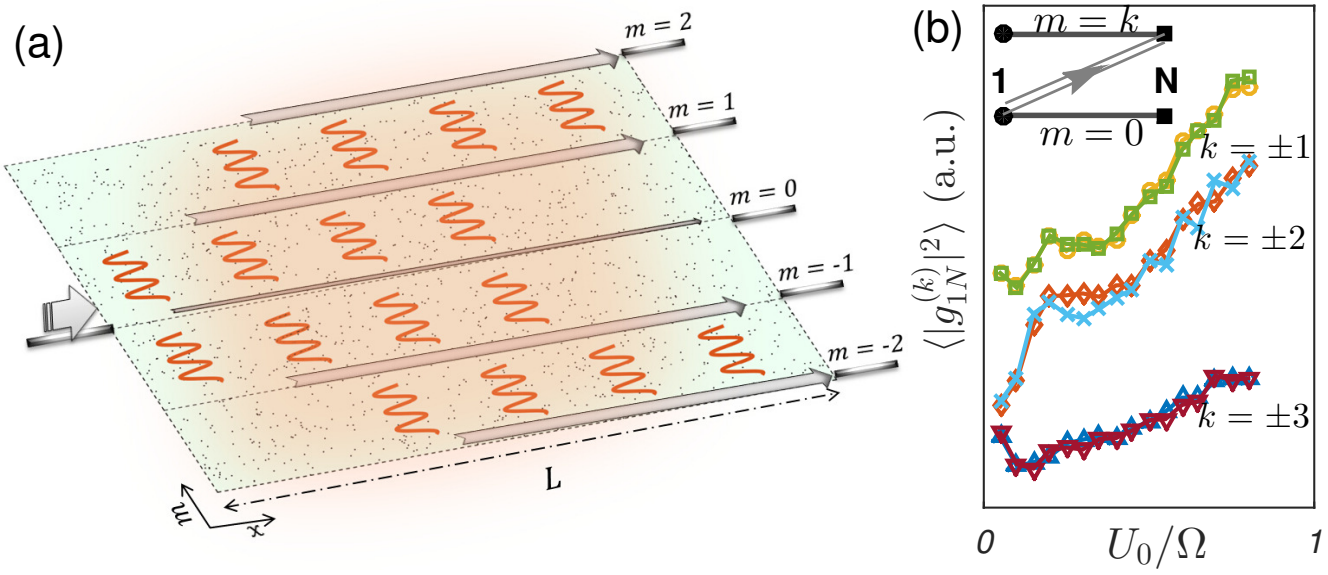

FIG. 4. **A schematic diagram illustrating the process by which transport is enhanced by disorder in the presence of light irradiation**. (a) Nonequilibrium transport through a two-terminal, light irradiated system with disorder. Electrons are injected from the left lead into the Floquet channel $m = 0$, pass the light irradiated scattering region, and exit the right lead through the Floquet channels $m = 0, \pm1, \pm2, \cdots$. The orange wave trains signify photon absorption and emission between adjacent Floquet channels and the gray arrows represent transport within the Floquet channels. (b) Surface Green's function g^k_{1N} describing the contact between slice 1 and N when k photons are absorbed in a closed nanoflake (inset).

impurities can contribute positively to the coupling and, consequently, enhance the transitions among the different Floquet states. In general, the increase in the conductance due to enhanced coupling is approximately proportional to U_0^2: $\langle G\rangle \approx \left(1 + |\alpha_\pm| U_0^2\right) G_{U_0=0}$. A simple fitting of this formula with the numerical results is shown as the green curve in Fig. 2(a).

The Born theory provides a mechanism by which the phenomenon of disorder enhanced transport under light irradiation can be understood. Specifically, Fig. 4(a) shows a schematic diagram of the transport process, where the levels m at different coordinate locations represent the Floquet channels and the short wave trains denote the photon absorption/emission process. For instance, for electrons injected into the Floquet channel $m = 0$ from the left lead, the probability of photon absorption/emission is enhanced by the disorder in the light-irradiated region. As a result, the transmission from channel $m = 0$ to channel k is enhanced, for $|k| > 1$, leading to an enhancement in the total conductance which is proportional to the sum of the transmission $T^{(k)}$.

Another speculative mechanism for transport enhancement is disorder induced breaking of the match between wavefunctions at the boundaries of the light-free and light-irradiated regions which, if true, would represent a correction to the Born theory. To test whether such a correction is necessary, we calculate, for a closed nanoflake, the surface Green's function $\mathcal{G}^k_{1N}$ for the transition from Floquet state $m = 0$ to state k, which is the block matrix

$$\mathcal{G}^F(z) = [z + i\eta - H^F]^{-1}$$

with its normalized form given by

$$g^k_{1N} = \mathcal{G}^k_{1N} / \sum_m \mathcal{G}^m_{1N}.$$

We use 10^3 sets of disorder realizations for each U_0 and calculate the average normalized surface Green's function. The results are shown in Fig. 4(b). We see that, as the disorder strength is increased, the function $g^{(k)}_{1N}(E)$ with $|k| > 1$ becomes more and more elevated. This rules out the boundary wavefunction matching as a possible contributing factor to disorder enhanced transport.

It should be noted that, although we have exploited the Born approximation to obtain the theoretical results, the finite-size Kubo formula[54] can also be used to obtain the same results. In particular, in the Kubo formula of linear response theory, the effective Hamiltonian of a finite Floquet system (e.g., a finite irradiated graphene nanoribbon) is the same as that used in the Green's function method. The Kubo formula can thus be used to predict the phenomenon of disorder-enhanced conductance.

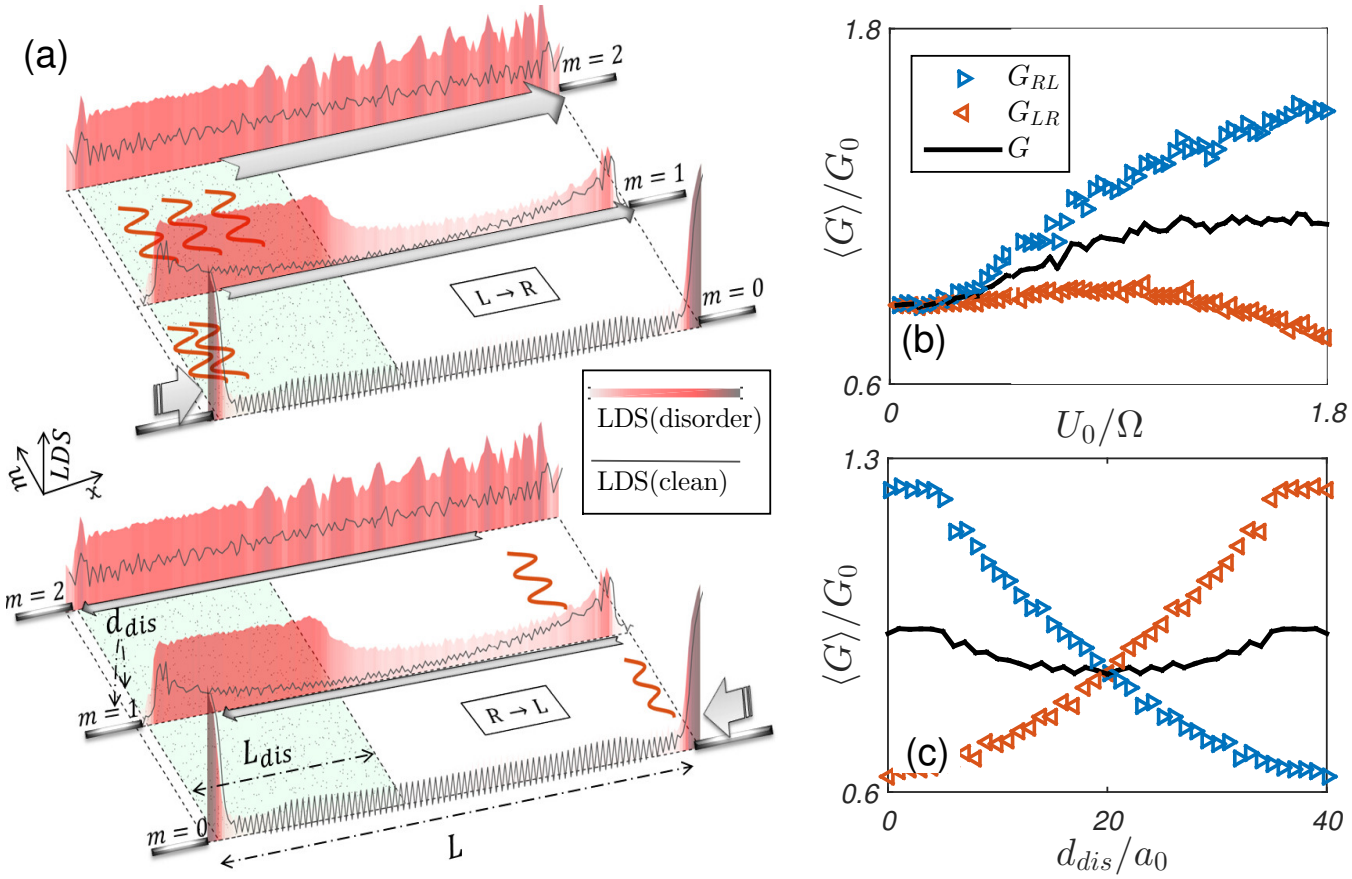

FIG. 5. **Asymmetric transport in a partially disordered system**. (a) A diagram schematically illustrating nonequilibrium transport in a two-terminal irradiated system in which disorder exists in part of the system only. The upper and lower diagrams are for $L \to R$ and $R \to L$ transport, respectively, L_{dis} is the length of the region containing disorder, and d_{dis} is the distance between the disordered region and the left lead. The LDS patterns in various Floquet channels are averaged by 100 disorder realizations for $U_0/\Omega = 1.6$, $L = 80a_0$, $L_{dis} = 30a_0$, and $d_{dis} = 2a_0$. (b) Average conductance versus the disorder strength for $\Omega = 0.8\gamma_0$, $A_0 = 0.15$, and $L_{dis} = 20a_0$ for a zigzag graphene ribbon of length $L = 70a_0$ and width $W = 50a$. (c) Average conductance versus the location of the disorder region for $L_{dis} = 30a_0$. The average conductance is calculated using 200 disorder realizations.

C. Asymmetrical transport in a partially disordered system

To test the generality of light mediated, disorder enhanced transport, we study the case in which random impurities exist only in part of the light irradiated scattering region. Concretely, we assume that impurities exist only in a subregion of length L_{dis}, which is at distance d_{dis} from the left lead, as shown in Fig. 5(a), where the upper and the lower panels represent the transport processes in the two opposite directions: $L \leftarrow R$ and $R \to L$, respectively. We examine the distribution of local density of states (LDS) in different Floquet channels. For the $m = 0$ channel, due to the wavefunction mismatching at the boundaries of the region with impurities, the LDS concentrates near the boundaries and assumes low values elsewhere. For this channel, the disorder has little effect on the transport. However, for channels $m = \pm 1$, LDS in the disordered region is greatly enhanced. Marked enhancement in the LDS distribution also occurs for higher Floquet channels ($|m| > 1$). The enhancement in the LDS for most Floquet channels is consistent with the theoretical prediction based on the Born approximation.

Figures 5(b) and 5(c) show, for the partially disordered system, the conductances associated with transport in the two opposite directions (i.e., $L \to R$ and $R \to L$) versus the disorder strength and the location of the impurity region, respectively. The striking phenomenon is a high degree of asymmetry in the conductances G_{LR} and G_{RL}: their values and trends of variation are drastically different. In particular, as shown in Fig. 5(b), the values of G_{RL} and G_{LR} gradually drift away from each other and their ratio can reach the value $G_{RL}/G_{LR} \approx 2$ as U_0 is increased. However, the average conductance $\langle G \rangle$, which takes into account transport in both directions, is enhanced only slightly by disorder. As the distance d_{dis}

is varied, the difference between G_{RL} and G_{LR} is modulated, as shown in Fig. 5(c), where the G_{RL} and G_{LR} versus d_{dis} curves exhibit a monotonously decreasing and increasing behavior, respectively and cross each other at the left-right symmetrical point $d_{dis} = 20a_0$.

While it is generally true that, for a driven system, the transport processes in the two opposite directions are not on equal footing[31], the highly asymmetric behavior in Figs. 5(b) and 5(c) involves an additional mechanism. In particular, we note that, for the Floquet channel $m = 0$, the conductance $G^{(0)}_{\beta\alpha}$ has small values due to its low LDS in most of the scattering region. As a result, for $L \to R$ transport, electrons injected into the left lead tend to accumulate there. Due to a larger overlapping area at the left side between the LDS patterns of the Floquet channels $m = 0$ and $m = \pm 1$, there is a high probability that the electrons transfer from the $m = 0$ to the $m = \pm 1$ channels. Similarly, the probabilities for electrons to transmit from the $m = \pm 1$ to higher Floquet channels are also appreciable. As a result, the conductances $G^{(|k|>0)}_{LR}$ are enhanced by impurities distributed near the left lead, as shown by the curved lines in Fig. 5(a). On the contrary, for the $R \to L$ transport, the overlap in the LDS between channels $m = 0$ and $m = \pm 1$ is insignificant, so fewer electrons can be transfered to higher channels, leading to a small conductance. We thus see that, an asymmetric distribution of the disorder in the light irradiated region can lead to a dramatic difference between the values of the conductances G_{RL} and G_{LR}. Our LDS based argument suggests that increasing the distance d_{dis} can reduce the conductance G_{RL} associated with $R \leftarrow L$ transport.

IV. DISCUSSION

A monolayer graphene subject to light irradiation can exhibit a class of quantum states that are not possible in the absence of light: topologically insulating Floquet states[13]. For a graphene nanoribbon of sufficient length such that the effects of evanescent states can be neglected, the Floquet states correspond to the distinct conducting channels. A proper level of random disorder promotes the transitions between the adjacent Floquet channels and, consequently, facilitates transport through the ribbon, leading to significant conductance enhancement. Qualitatively, the conductance as a function of the disorder strength can exhibit a resonance-like behavior: the conductance increases as the disorder strength is increased from zero, reaches maximum for an optimal value of the disorder strength, and decreases as disorder is further strengthened. The improvement in the conductance is quite remarkable: the ratio between the maximum value and its value for zero disorder can reach the value of about 1.5. The resonance phenomenon is quite robust: it persists even when only part of the ribbon region is doped with impurities (although the extent of conductance enhancement is not as large as that for the case where the whole ribbon region is doped). Quantitatively, the resonance phenomenon can be explained by resorting to the Born approximation.

The resonance phenomenon uncovered in this paper has an origin that is distinct from that reported in previous works without any external time periodic driving[39,40], which is generated by the breaking of the edge states in a graphene nanoribbon through random scattering. Here, the physical mechanism for the resonance is disorder enhanced coupling between the adjacent Floquet channels that are created by light irradiation. The conductance enhancement associated with the resonance is thus a result of the interplay between light and disorder, implying, counterintuitively, that the response of graphene to light can be enhanced through random disorder. This may find applications in graphene based optoelectronics.

We remark that the physical mechanism for the resonance phenomenon is quite distinct from the traditional photon absorption process associated with interband transitions. In a system free of disorders, the Floquet state is in fact a light-dressed state and the irradiated light serves to change the trivial transmission mode to a non-trivial one. In particular, say we compare the irradiation-free system to that with irradiation at the Fermi energy $\varepsilon = \Omega/2$. Without irradiation, there is one trivial mode in the graphene nanoribbon with transmission one. However, the mode is not robust against impurities. In the presence of light radiation, a gap is opened at $\varepsilon = \Omega/2$, making the mode disappear, but a non-trivial edge state can arise, the Floquet topological edge state, which is topologically protected and is robust against disorder. The decay length of the evanescent states from the leads is determined by the gap size in the band structure. The Born theory stipulates that disorder can effectively reduce or even eliminate the light-induced gap, stretch the "tails" of the evanescent states and, consequently, enhance the transport. In the light-irradiated Floquet system, there are then two main contributing factors to the conductance: topologically protected edge and evanescent states. Disorder can enhance transport associated with the latter and but will not affect the transport due to the former. The physics of the Floquet states is thus distinct from that of the photon absorption process associated with interband transitions. These considerations suggest that direct absorption of electromagnetic radiation contributes little to the observed conductance enhancement.

We discuss the feasibility of experimental observation of the resonance phenomenon uncovered in our paper in terms of the two key requirements: laser irradiation and disorder tuning. For the irradiated laser in Fig. 2, the

value of frequency Ω corresponds to the wavelength of 3.6μm, and the value of A_0 requires a laser with power $0.2\text{mW}/\mu\text{m}^2$. Such lasers are readily available (e.g., infrared lasers), insofar as the frequency satisfies the inequality $\hbar\Omega < \gamma_0$ or the wavelength is larger than 2.88μm. As for disorders, there are experimental methods to tune their strength. For example, the strength can be controlled through modifying the density of electric charge doping in an insulated substrate or through ion irradiation on graphene surface. Irradiation of gallium ions can change the disorder strength up to 1.5 eV with little effect on the graphene electric structure[55]. If the graphene ribbon is prepared by chemical vapor deposition[56], impurities can be doped during the preparation process and the disorder strength can be tuned through controlling the doping elements and their densities. We thus expect that the resonance phenomenon to be experimentally observable.

ACKNOWLEDGEMENT

We thank Dr. L. E. F. Foa Torres for helpful discussions. We would like to acknowledge support from the Vannevar Bush Faculty Fellowship program sponsored by the Basic Research Office of the Assistant Secretary of Defense for Research and Engineering and funded by the Office of Naval Research through Grant No. N00014-16-1-2828. L.H. was supported by NNSF of China under Grant No. 11775101.

Appendix A: Floquet Green's function

The time-dependent Schrödinger equations for an irradiated system connected with leads are

$$\begin{aligned}\left[H(t)-i\frac{\partial}{\partial t}-i\Gamma/2\right]|\Phi_\alpha(t)\rangle &= (\varepsilon_\alpha - i\eta_\alpha)\,|\Phi_\alpha(t)\rangle \\ \left[H(t)-i\frac{\partial}{\partial t}+i\Gamma/2\right]|\widetilde{\Phi}_\alpha(t)\rangle &= (\varepsilon_\alpha + i\eta_\alpha)\,|\widetilde{\Phi}_\alpha(t)\rangle\end{aligned} \tag{A1}$$

where the self-energy Γ describes the effects of leads[57]. The imaginary part of the eigenenergy, η_α, represents the decay rate of the quantum states into the semi-infinite leads. Due to the time periodicity, the wavefunction can be written as

$$|\Phi_\alpha(t)\rangle = \sum_{m=-\infty}^{+\infty} e^{im\Omega t}|\varphi_\alpha^m\rangle, \tag{A2}$$

where $|\phi_\alpha^m\rangle$ is time independent. The time dependent terms in Eq. (A1) can be eliminated by utilizing Eq. (A2) through an integral over a period of external driving. The original time dependent system can then be transformed into the following time independent system:

$$\begin{aligned}[\varepsilon_\alpha - i\eta_\alpha + n\Omega - i\Gamma/2]\,|\varphi_\alpha^n\rangle &= \sum_m (H_{n-m})\,|\varphi_\alpha^m\rangle \\ [\varepsilon_\alpha + i\eta_\alpha + n\Omega + i\Gamma/2]\,|\widetilde{\varphi}_\alpha^n\rangle &= \sum_m (H_{n-m})\,|\widetilde{\varphi}_\alpha^m\rangle,\end{aligned} \tag{A3}$$

where

$$H_n = (1/T)\int_0^T H(t)\exp[in\Omega t]dt.$$

The Floquet Green's function is given by

$$\mathcal{G}_n = \sum_\alpha \sum_m \frac{|\varphi_\alpha^{n-m}\rangle\langle\widetilde{\varphi}_\alpha^m|}{E-\varepsilon_\alpha+i\eta_\alpha-m\Omega}. \tag{A4}$$

In numerical calculations, a matrix framework is desired. The retarded Green's function of the whole system can be written as

$$\boldsymbol{G}^r = \frac{\boldsymbol{I}}{E+i\eta+\boldsymbol{\Omega}-\boldsymbol{H}-i\boldsymbol{\Gamma}/2}, \tag{A5}$$

where

$$\boldsymbol{H} = \begin{pmatrix} \ddots & \vdots & \vdots & \vdots & \\ \cdots & H_0 & H_1 & & \\ \cdots & H_{-1} & H_0 & H_1 & \cdots \\ & & H_{-1} & H_0 & \cdots \\ & \vdots & \vdots & \vdots & \ddots \end{pmatrix}, \quad \boldsymbol{\Gamma} = \begin{pmatrix} \ddots & & & & \\ & \Gamma(E+\Omega) & & & \\ & & \Gamma(E) & & \\ & & & \Gamma(E-\Omega) & \\ & & & & \ddots \end{pmatrix},$$

$$\boldsymbol{\Omega} = \begin{pmatrix} \ddots & & & & \\ & +1\Omega & & & \\ & & 0 & & \\ & & & -1\Omega & \\ & & & & \ddots \end{pmatrix}, \quad \boldsymbol{G} = \begin{pmatrix} \ddots & \vdots & \vdots & \vdots & \\ \cdots & \mathcal{G}_{11} & \mathcal{G}_{01} & \mathcal{G}_{-11} & \cdots \\ \cdots & \mathcal{G}_{10} & \mathcal{G}_{00} & \mathcal{G}_{-10} & \cdots \\ \cdots & \mathcal{G}_{1-1} & \mathcal{G}_{0-1} & \mathcal{G}_{-1-1} & \cdots \\ & \vdots & \vdots & \vdots & \ddots \end{pmatrix}, \tag{A6}$$

and $\mathcal{G}_{0k} \equiv \mathcal{G}^{(k)}$. We use the recursive Green's function scheme in numerical computations[58,59]. Finally, the quantum transmission is given by

$$T^k_{\nu\mu}(E) = Tr[\Gamma^{(k)}_\nu \mathcal{G}^{(k)}_{1N}(E)\Gamma^{(0)}_\mu \mathcal{G}^{(k)\dagger}_{1N}(E)], \tag{A7}$$

where $\mu(\nu) = L, R$.

Appendix B: Born approximation

We provide a theoretical understanding of the phenomenon of disorder-enhanced coupling by resorting to the first-order Born approximation which is valid in the low energy regime. In our simulations within the tight-binding framework [Eqs. (1) and (3)], the frequency Ω of the irradiated field is smaller than the bandwidth of the system. As a result, a resonance (topological gap) can emerge at both integer and half-integer times of the frequency. To gain insights into the essential physics, we focus on the case of a single resonance. The effective Hamiltonian containing two diagonal Floquet blocks can be written as

$$H^F = \begin{pmatrix} H_{\text{eff}} + \Omega & V_+ \\ V_- & H_{\text{eff}} \end{pmatrix}, \tag{B1}$$

with

$$H_{\text{eff}} = \begin{pmatrix} \Delta_0 & k_- \\ k_+ & -\Delta_0 \end{pmatrix}. \tag{B2}$$

The two Floquet blocks are coupled with each other by V_+ and V_-, where $k_\pm = k_x \pm ik_y$ and $\Delta_0 = v_F^2 A_0^2/\Omega$ is the topological mass. In the absence of disorder, the Floquet Green's function is

$$G^F_0(z, \mathbf{k}) = [z - H^F(\mathbf{k})]^{-1}. \tag{B3}$$

The disorder potential in the real space can then be written as

$$U_{dis}(\mathbf{r}) = \sum_i \begin{pmatrix} u^A_i \delta(\mathbf{r} - \mathbf{r}^A_i) & 0 \\ 0 & u^B_i \delta(\mathbf{r} - \mathbf{r}^B_i) \end{pmatrix}, \tag{B4}$$

where $u^{A,B}_i$ are uniformly distributed in the range $[-U_0/2, U_0/2]$ and satisfy the relations

$$\langle u^{A,B}_i \rangle = 0, \tag{B5}$$

$$\langle u^s_i u^{s'}_j \rangle = \tfrac{U_0^2}{12} \delta_{ij}\delta_{ss'}, \tag{B6}$$

with $s, s' = A, B$. Using the Floquet Green's function and the disorder potential expressions, we obtain

$$\Sigma_{dis}(z, \mathbf{k}) = \int_{FBZ} d\mathbf{k}' \langle U_{dis}(\mathbf{k}, \mathbf{k}') G^F_0(z, \mathbf{k}') U_{dis}(\mathbf{k}', \mathbf{k}) \rangle, \tag{B7}$$

where the approximations $A_0 \ll 1$ are used. The off diagonal block of the effective Hamiltonian $\widetilde{H}^F = H^F + \Sigma_{dis}$ can be written as

$$\widetilde{V}_+ = \begin{pmatrix} 0 & 0 \\ A_0 + \widetilde{A}_+ & 0 \end{pmatrix}, \quad \widetilde{V}_- = \begin{pmatrix} 0 & A_0 + \widetilde{A}_- \\ 0 & 0 \end{pmatrix}, \tag{B8}$$

where

$$\widetilde{A}_\pm = A_0 \left(1 + \alpha_\pm U_0^2\right), \tag{B9}$$

and

$$\alpha_\pm = -\frac{\Omega}{12} \int_{FBZ} \frac{k_\pm d\mathbf{k}}{(k_+k_- + \Delta_0^2)(k_+k_- + \Delta_0^2 - \Omega^2)}. \tag{B10}$$

* Ying-Cheng.Lai@asu.edu

[1] A. B. Kuzmenko, E. van Heumen, F. Carbone, and D. van der Marel, Phys. Rev. Lett. **100**, 117401 (2008).
[2] L. A. Falkovsky, J. Phys. Conf. Ser. **129**, 012004 (2008).
[3] M. K. Kavitha and M. Jaiswal, Asian J. Phys. **25**, 809 (2016).
[4] R. Binder, *Optical Properties of Graphene*, 1st ed. (World Scientific, Singapore, 2017).
[5] R. Benzi, A. Sutera, and A. Vulpiani, J. Phys. A **14**, L453 (1981).
[6] R. Benzi, G. Parisi, A. Sutera, and A. Vulpiani, J. Appl. Math. **43**, 565 (1983).
[7] B. McNamara and K. Wiesenfeld, Phys. Rev. A **39**, 4854 (1989).
[8] F. Moss, D. Pierson, and D. O'Gorman, Int. J. Bif. Chaos **4**, 1383 (1994).
[9] P. C. Gailey, A. Neiman, J. J. Collins, and F. Moss, Phys. Rev. Lett. **79**, 4701 (1997).
[10] L. Gammaitoni, P. Hänggi, P. Jung, and F. Marchesoni, Rev. Mod. Phys. **70**, 223 (1998).
[11] Z. Liu and Y.-C. Lai, Phys. Rev. Lett. **86**, 4737 (2001).
[12] K. Park, Y.-C. Lai, and S. Krishnamoorthy, Phys. Rev. E **75**, 046205 (2007).
[13] T. Oka and H. Aoki, Phys. Rev. B **79**, 081406 (2009).
[14] T. Kitagawa, T. Oka, A. Brataas, L. Fu, and E. Demler, Phys. Rev. B **84**, 235108 (2011).
[15] Z. Gu, H. A. Fertig, D. P. Arovas, and A. Auerbach, Phys. Rev. Lett. **107**, 216601 (2011).
[16] H. L. Calvo, H. M. Pastawski, S. Roche, and L. E. F. Foa Torres, Appl. Phys. Lett. **98**, 232103 (2011).
[17] L. E. F. Foa Torres, P. M. Perez-Piskunow, C. A. Balseiro, and G. Usaj, Phys. Rev. Lett. **113**, 266801 (2014).
[18] P. M. Perez-Piskunow, G. Usaj, C. A. Balseiro, and L. E. F. F. Torres, Phys. Rev. B **89**, 121401 (2014).
[19] M. C. Rechtsman, Y. Plotnik, J. M. Zeuner, D. Song, Z. Chen, A. Szameit, and M. Segev, Phys. Rev. Lett. **111**, 103901 (2013).
[20] Y. Lumer, Y. Plotnik, M. C. Rechtsman, and M. Segev,

Phys. Rev. Lett. **111**, 243905 (2013).
[21] P. M. Perez-Piskunow, L. E. F. Foa Torres, and G. Usaj, Phys. Rev. A **91**, 043625 (2015).
[22] A. Kundu, H. A. Fertig, and B. Seradjeh, Phys. Rev. Lett. **113**, 236803 (2014).
[23] V. Dal Lago, M. Atala, and L. E. F. Foa Torres, Phys. Rev. A **92**, 023624 (2015).
[24] M. Busl, G. Platero, and A.-P. Jauho, Phys. Rev. B **85**, 155449 (2012).
[25] Y. T. Katan and D. Podolsky, Phys. Rev. Lett. **110**, 016802 (2013).
[26] G. Usaj, P. M. Perez-Piskunow, L. E. F. Foa Torres, and C. A. Balseiro, Phys. Rev. B **90**, 115423 (2014).
[27] P. Titum, N. H. Lindner, M. C. Rechtsman, and G. Refael, Phys. Rev. Lett. **114**, 056801 (2015).
[28] A. Kundu, H. A. Fertig, and B. Seradjeh, Phys. Rev. Lett. **116**, 016802 (2016).
[29] M. Sentef, M. Claassen, A. Kemper, B. Moritz, T. Oka, J. Freericks, and T. Devereaux, Nat. Commun. **6** (2015).
[30] Y. H. Wang, H. Steinberg, P. Jarillo-Herrero, and N. Gedik, Science **342**, 453 (2013).
[31] S. Kohler, J. Lehmann, and P. Hänggi, Phys. Rep. **406**, 379 (2005).
[32] M. Katsnelson, Eur. Phys. J. B **51**, 157 (2006).
[33] J. H. Bardarson, J. Tworzydło, P. W. Brouwer, and C. W. J. Beenakker, Phys. Rev. Lett. **99**, 106801 (2007).
[34] M. Titov, EPL (Europhys. Lett.) **79**, 17004 (2007).
[35] A. Rycerz, J. Tworzydło, and C. Beenakker, EPL (Europhys. Lett.) **79**, 57003 (2007).
[36] R. Akis, D. K. Ferry, and J. P. Bird, Phys. Rev. Lett. **79**, 123 (1997).
[37] G. Wang, L. Ying, and Y.-C. Lai, Phys. Rev. E **92**, 022901 (2015).
[38] L. Ying, L. Huang, Y.-C. Lai, and C. Grebogi, Phys. Rev. B **85**, 245448 (2012).
[39] W. Long, Q.-F. Sun, and J. Wang, Phys. Rev. Lett. **101**, 166806 (2008).
[40] L.-L. Jiang, L. Huang, R. Yang, and Y.-C. Lai, Appl. Phys. Lett. **96**, 262114 (2010).
[41] L. Ying and Y.-C. Lai, Phys. Rev. B **96**, 165407 (2017).
[42] R. A. Jalabert., H. U. Baranger, and A. D. Stone, Phys. Rev. Lett. **65**, 2442 (1990).
[43] Y.-C. Lai, R. Blümel, E. Ott, and C. Grebogi, Phys. Rev. Lett. **68**, 3491 (1992).
[44] R. Ketzmerick, Phys. Rev. B **54**, 10841 (1996).
[45] A. S. Sachrajda, R. Ketzmerick, C. Gould, Y. Feng, P. J. Kelly, A. Delage, and Z. Wasilewski, Phys. Rev. Lett. **80**, 1948 (1998).
[46] B. Huckestein, R. Ketzmerick, and C. H. Lewenkopf, Phys. Rev. Lett. **84**, 5504 (2000).
[47] R. Yang, L. Huang, Y.-C. Lai, and C. Grebogi, EPL (Europhys. Lett.) **94**, 40004 (2011).
[48] R. Yang, L. Huang, Y.-C. Lai, and L. M. Pecora, Appl. Phys. Lett. **100**, 093105 (2012).
[49] G. L. Wang, L. Ying, Y.-C. Lai, and C. Grebogi, Phys. Rev. E **87**, 052908 (2013).
[50] R. Yang, L. Huang, Y.-C. Lai, C. Grebogi, and L. M. Pecora, Chaos **23**, 013125 (2013).
[51] L. Ying, G. Wang, L. Huang, and Y.-C. Lai, Phys. Rev. B **90**, 224301 (2014).
[52] K. Kobayashi, T. Ohtsuki, and K.-I. Imura, Phys. Rev. Lett. **110**, 236803 (2013).
[53] I. C. Fulga and M. Maksymenko, Phys. Rev. B **93**, 075405 (2016).
[54] K. Nomura and A. H. MacDonald, Phys. Rev. Lett. **98**, 076602 (2007).
[55] Y.-B. Zhou, Z.-M. Liao, Y.-F. Wang, G. S. Duesberg, J. Xu, Q. Fu, X.-S. Wu, and D.-P. Yu, The Journal of chemical physics **133**, 234703 (2010).
[56] D. Wei, Y. Liu, Y. Wang, H. Zhang, L. Huang, and G. Yu, Nano letters **9**, 1752 (2009).
[57] M. L. Sancho, J. L. Sancho, J. L. Sancho, and J. Rubio, J. Phys. F Metal Phys. **15**, 851 (1985).
[58] H. L. Calvo, P. M. Perez-Piskunow, H. M. Pastawski, S. Roche, and L. E. F. Torres, J. Phys. Conden. Mat. **25**, 144202 (2013).
[59] L. Ying, L. Huang, Y.-C. Lai, and Y. Zhang, J. Phys. Conden. Mat. **25**, 105802 (2013).